ACS Photonics

Letter

pubs.acs.org/journal/apchd5

Bending-Induced Bidirectional Tuning of Whispering Gallery Mode Lasing from Flexible Polymer Fibers

Rui Chen,[†] Van Duong Ta,[†] and Handong Sun*[,†,‡]

[†]Division of Physics and Applied Physics, School of Physical and Mathematical Sciences, Nanyang Technological University, Singapore 637371, Singapore

[‡]Centre for Disruptive Photonic Technologies (CDPT), Nanyang Technological University, Singapore 637371, Singapore

Supporting Information

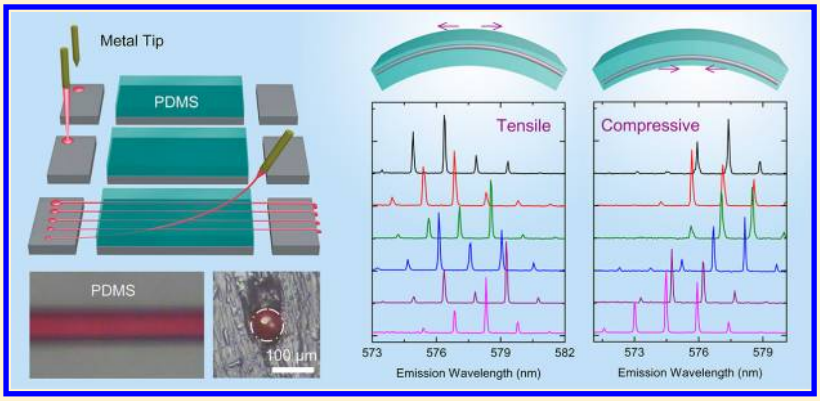

ABSTRACT: Polymer microfibers with a circular cross-section are directly drawn from a solution. By encapsulating the dye-doped microfibers with polydimethylsiloxane (PDMS) elastomer, optically pumped lasing with enhanced photostability is achieved. The lasing characteristics as well as size-dependent lasing action are carefully analyzed, and the lasing phenomenon is ascribed to whispering gallery mode. The PDMS elastomer offers another degree of freedom to mechanically tune the lasing from microfibers. It is interesting to note that by different types of bending, bidirectional shifting of the laser wavelength is observed, which is due to strain-induced refractive index change of the fiber and PDMS matrix. Our studies not only show an effective method to passivate the microfibers, but also open up a new approach to manipulating the lasing, which allows for fine adjustment of laser emission to any desired wavelength within the tuning range.

KEYWORDS: *microlasers, tunable, whispering gallery mode, strain, flexible microfibers*

With the rapid development of nanoscience and nanotechnology, various types of microresonators have been proposed and demonstrated, such as the Fabry-Pérot cavity,[1,2] distributed feedback (DFB) grating,[3] photonic crystal,[4] random cavity,[5−7] whispering gallery mode (WGM),[8−10] and combination with plasmonic resonances for nanosized laser sources.[11−14] This is motivated by both the fundamental interest of cavity-induced change of the spontaneous emission,[15] and the potential applications as microlasers,[16] detectors, and ultrasensitive sensors.[17] WGM resonance in a circular microcavity always possesses a high quality (Q) factor as well as small mode volume and, therefore, has attracted intensive research attention.[18,19] Besides microdisks,[9] micropillars,[20] spheres,[21,22] and hemispheres,[23−25] active cylindrical wires or fibers represent attractive candidates because they hold the potential to be used as a laser source and a waveguide simultaneously.[13,26,27]

Besides the high quality performance, integrated photonics applications also require microlasers to be cheap, stable, flexible, and highly tunable. Recently, significant progresses have been made on organic single nanowire or nanofibers for subwavelength multicolor light sources,[28] waveguides,[26,27] and optically pumped lasers.[29] Compared to semiconductors, polymer fibers might be favorable because they can be easily doped with functional materials. Moreover, they are less costly and easier for material fabrication and device processing. Very recently, WGM lasing from dye-doped polymer fibers had been realized, and the proof-of-concept refractive index sensing was demonstrated.[30,31] However, due to the photo-oxidation effect, frequency shifting and mode hopping were generally observed in dye molecules or colloidal quantum dots (QDs) doped systems, which strongly affect the stability and reliability of these devices.[22,24,32,33]

On the other hand, tunable lasing still remains the ultimate scientific goal, which is driving enormous efforts to address the relevant challenges. As is well-known, lasing emissions are sensitive to the gain medium, refractive index, and optical cavity size.[34] To date, different methods have been proposed to tune

Received: October 22, 2013
Published: January 6, 2014

   dx.doi.org/10.1021/ph400084s | *ACS Photonics* 2014, 1, 11−16

the wavelength of lasers.[16,35−41] Examples include the electrically tunable liquid crystal microlaser,[35] optically tunable organic laser,[36] mechanically tunable optofluidic DFB laser,[37,42] and so on.

In order to address the problems of stability and tunability as mentioned above, we proposed herein to place the polymer fiber inside polydimethylsiloxane (PDMS) elastomer. PDMS was chosen because of its transparency, low refractive index, and good mechanical properties. It is found that the polymer fibers into PDMS can still maintain their high quality WGM lasing, which is confirmed by power-dependent and size-dependent measurements. As expected, the photostability of the lasing emission is significantly improved. More interestingly, the elastomer matrix enables us to mechanically tune the lasing emission. By bending the fibers, bidirectional tuning of WGM lasing wavelength can be achieved. The mechanism is ascribed to the refractive index change of both the fiber and PDMS matrix. This feature would launch a wide range of novel applications.

The polymer fibers were fabricated from modified solution as reported previously.[30] The solution is a mixture of polymethylmethacrylate (PMMA) with dichloromethane of concentration of 11 wt %. Organic dye molecules Rhodamine 6G (R6G) and Araldite 506 epoxy resins, purchased from Sigma-Aldrich, were doped into the solution. The concentration of R6G is around 0.12 wt % and the weight ratio between the PMMA and epoxy resin is 1:2. It should be mentioned that adding high viscous epoxy resin slows down the evaporation of solvent and fibers with smooth outer surface can be readily achieved. A JEOL JSM-7001F field emission scanning electron microscope (FESEM) was used to characterize the morphology of the sample. For optical measurements, the laser source was a frequency-doubled, Q-switched Nd:YAG laser emitted at 532 nm. The pulse width and repetition rate of the laser are 1 ns and 60 Hz, respectively. The laser beam was guided at a grazing angle ∼45° normal to the sample placed on an X−Y−Z movable stage. The polarization direction of the laser beam is along the microfiber. The signal emitted from the fiber was collected with an objective (50× , numerical aperture = 0.42), directed into a 750 mm monochromator and detected by a back-illuminated silicon charged coupled device (CCD) for spectral. Proper filters were placed in front of the entrance slit of the monochromator, and a variable-density attenuator was used to adjust the power of the excitation. Schematic diagram of the measurement setup can be found in Figure S1.

Figure 1a shows the diagram of directly drawing polymer fibers from the composite solution. The PDMS (Sylgard 184 Silicon Elastomer from Dow Corning) was prepared by mixing a 10:1 mass ratio of liquid silicon base and a curing agent. To create polymer fibers, a drop of solution was placed on the substrate. A sharp metal tip was immersed into the drop and then pulled out with a constant speed. The fiber was guided across the uncured PDMS. Due to the gravity, polymer fiber will sink gradually inside PDMS matrix. As indicated in the figure, by changing the size or the drawing speed of the metal tip, polymer fiber with different sizes can be obtained. After fabrication, the structure was left at room temperature for about two days for solidification. The fiber in PDMS maintains its bright red color, as shown in Figure 1b, which indicates that no deterioration of gain medium occurs during the curing process. Due to the flexibility, we are able to cut the fiber and check its cross-section. From the optical image shown in Figure 1c, it can be clearly seen that the polymer fiber has a circular shape. In addition, polymer fiber which is not covered by PDMS has been measured. The FESEM image shown in Figure S2 indicates a smooth outer surface and uniform size along the fabricated fiber.

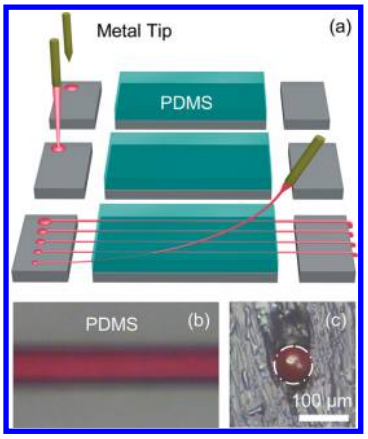

Figure 1. (a) Schematic diagram shows the fabrication of polymer fiber in PDMS by direct drawing. (b) Optical image of the fiber inside PDMS. (c) Cross-section of the fiber in PDMS where the circle indicates the position of fiber.

Figure 2a plots the power-dependent photoluminescence (PL) measurement of a typical single polymer fiber with radius about 33 μm. Two distinct regions can be clearly seen. For pump pulse energy below the threshold (∼0.97 μJ), weak and broad spontaneous emission from the fiber is observed. At threshold, initial sharp peaks emerge from the broad emission, as shown in Figure S3. Above threshold, those peaks increase rapidly with the pump pulse energy. A plot of integrated PL intensity of the peaks with pump pulse energy is presented in the inset of Figure 2a. The clear transition from spontaneous emission to stimulated emission and the nonlinear increase of the emission intensity indicate the lasing phenomenon. Figure 2b−d shows the optical image of the measured polymer fiber. It is noted that above threshold (Figure 2d), the emission from the fiber is much brighter compared with the one below threshold (Figure 2c). Moreover, above threshold, bright emission from the edge of the fiber can be observed. This predicts the cavity of the lasing may come from WGM, which is benefited from the circular shape and smooth interface of the microfiber.

As mentioned above, frequency shifting and mode hopping are generally observed in dye or colloidal QD-doped flexible microlasers.[22,24,43] This nonreversible blueshift of the lasing peak comes from the slight change of cavity size and the photo-oxidation of the gain medium. This issue ruins many potential applications based on the polymer fibers. An effective method to solve this problem is to cure and isolate the gain medium from oxygen, as proposed in our work. The mapping of normalized lasing peaks with pump pulse energy is plotted in Figure 2e. The straight lines indicate that all the lasing peaks maintain at identical position during optical pumping, which implies good passivation of the polymer fiber in PDMS matrix.

The lasing mechanism is further confirmed by analyzing the lasing characteristics. In spherical microcavities, the light is trapped inside the microstructure by total internal refraction between the microstructure (n_1) and the surrounding medium (n_2), where $n_1 > n_2$. The lasing modes can be predicted from the following equation.[44,45]

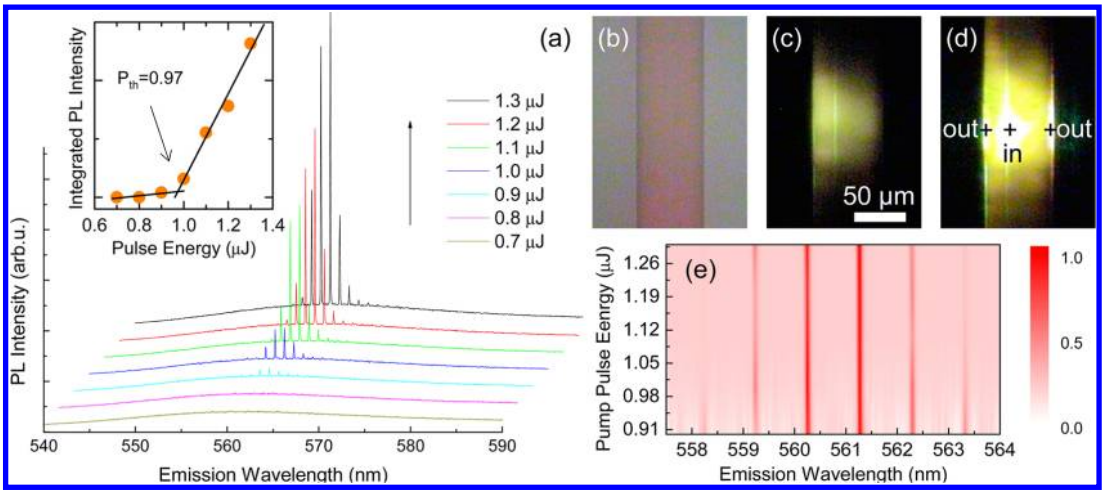

Figure 2. (a) Power-dependent PL measurement of single polymer fiber. Inset shows the integrated PL intensity with pulse energy. (b–d) Optical images of the measured fiber below (c) and above (d) lasing threshold; "in" denotes the spot of laser excitation, while "out" indicates the laser output from the rim of the microfiber. (e) Mapping of the normalized lasing emission with pump pulse energy.

$$\lambda^{-1}(R, n_1, n_r, r, m) = \frac{1}{2\pi R n_1}\left[m + \frac{1}{2} + 2^{-1/3}a(r)\left(m + \frac{1}{2}\right)^{1/3} - \frac{L}{(n_r^2 - 1)^{1/2}} + \frac{3}{10}2^{-2/3}a^2(r)\left(m + \frac{1}{2}\right)^{-1/3} - 2^{-1/3}L\left(n_r^2 - \frac{2}{3}L^2\right)\frac{a(r)\left(m + \frac{1}{2}\right)^{-2/3}}{(n_r^2 - 1)^{3/2}}\right] \quad (1)$$

where R is the radius of the circular microcavity, $n_r = n_1/n_2$, $L = 1/n_r$ for transverse magnetic (TM) modes, and $L = n_r$ for transverse electric (TE) modes, $a(r)$ is the roots of the Airy function where r is the radial mode number, and m is the mode number. If we insert R = 33.5 μm, refractive index 1.475 and 1.411 for polymer fiber (n_1) and PDMS (n_2),[21] the lasing peaks can be well-fitted, as shown in Figure 3. Theoretical calculation implies that the lasing peaks belong to first order (r = 1) TM modes, and the corresponding mode numbers count from 538 to 544. The line width ($\Delta\lambda$) of the lasing peak is small, which is around 0.07 nm. According to $Q = \lambda/\Delta\lambda$, the cavity Q-factor is estimated to be around 7800. Actually, the Q-factor for fiber in PDMS is smaller than the one in air, which is due to the lower refractive index contrast. Nevertheless, thanks to the lower refractive index of PDMS than polymer fiber, the fibers inside it still possible to support lasing emission. More importantly, it is well-protected against photo-oxidation.

To obtain more information about the lasing characteristics, a size-dependent measurement was conducted on individual polymer fibers. Figure 4a plots a series of lasing spectra detected from polymer fiber with different radius. It is found that the lasing always happen in the spectral region highlighted in the inset of Figure 4a. It can be seen that the position where gain is larger than the loss is located around the emission peak. Previous investigations show that the free spectral range (FSR) and Q-factor strongly depends on the size of a WGM cavity. As shown in Figure 4b, the FSR can be well-fitted by a/R, where a is a constant. This is reasonable because $FSR = \lambda^2/(n_{eff}\pi 2R)$, where λ is the resonant wavelength and n_{eff} is effective refractive index of fiber.[46] Moreover, the determined Q-factor is in the range of 5000 to 8000, which shows linear relation with the size of the fiber. Information about the optical image of fiber with different sizes can be found in Figure S4. We did not observe single longitudinal mode lasing from smaller fiber in PDMS. It should, however, be possible to obtain single-mode lasing under higher pump pulse energy. To conclude, the discussions above confirm that the lasing mechanism is due to WGM.

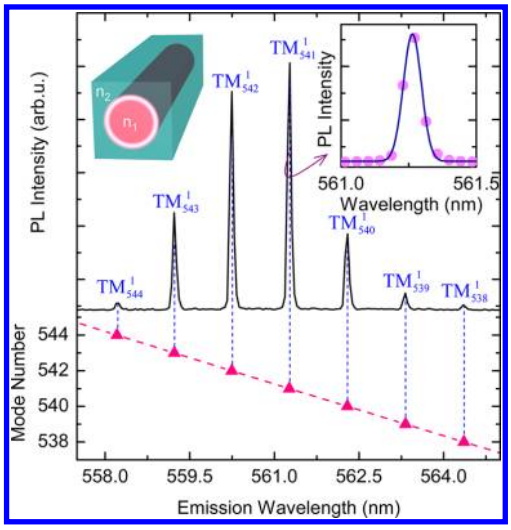

Figure 3. Lasing spectra from the polymer fiber in PDMS. The mode numbers and peak positions are determined from eq 1. Insets show the schematic diagram of the WGM in fiber and the magnification of one lasing peak.

In addition to the easy curing and good transparence, PDMS shows a good elastic property which is soft and deformable with no shrinkage. It therefore offers us another degree of freedom to modify the structure. It is known that strain is a useful tool to modulate the physical properties of materials. Strain tuning is usually realized by applying a mechanical force to either compress or stretch the structures. Up until now, most of the tunable flexible lasers are based on the strain-induced deformation of cavity or microstructures.[21,37,38,41,42] As will be presented later, mechanical bending is also an effective method to manipulate microlasers.

dx.doi.org/10.1021/ph400084s | ACS Photonics 2014, 1, 11–16

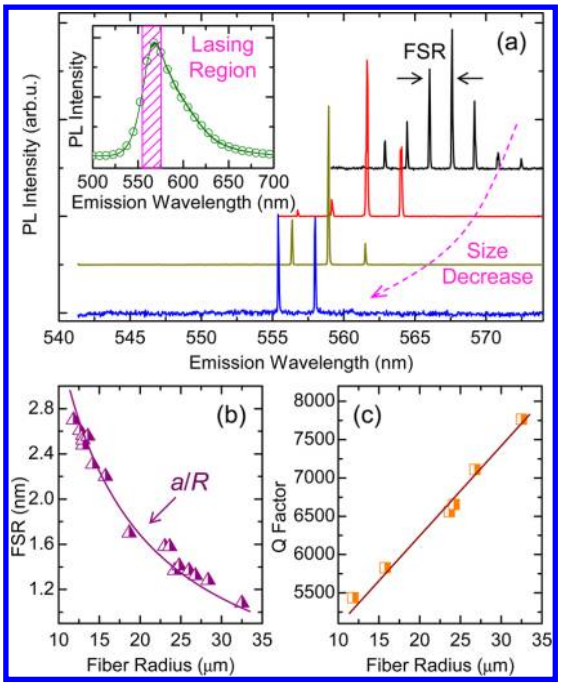

Figure 4. (a) WGM lasing from fiber inside PDMS with radius of 21.5, 13.7, 13.5, and 13.0 μm, respectively. Inset shows the spontaneous emission from the fiber and the highlighted area indicates the lasing region. (b) The FSR as a function of fiber's radius, fitted by a $1/R$ function. (c) The Q-factor from the fiber with various sizes show linear dependence of the fiber's radius.

As schematically show in Figure 5a, the fiber in PDMS was cut, with one end fixed to the substrate, while another end fixed to a moveable stage. The length and the thickness of the PDMS elastomer are 2 cm and 0.7 mm, respectively. Due to the force and the flexibility, when the stage is moving toward the fixed one, PDMS elastomer will bend upward automatically. The curvature increases with the moving ΔL. One polymer fiber with radius of around 23 μm was chosen and its cross-section was shown in Figure 5b,c. It is found that the fiber is located near one surface (Side A) of the PDMS. The microfiber was optically pumped and the emission was collected from the top side. By bending and tracing the lasing emission, interesting phenomenon has been observed. As shown in Figure 5g, when Side A is on top, a clear blueshift of lasing peaks can be observed by the bending (Figure 5d). Surprisingly, if Side B is on the top and bend the structure (Figure 5h), a continuous redshift of the peaks was obtained (Figure 5e). Comparing the measured spectrum, the total amount of shifting is larger than the peak spacing (FSR). During the bending, no higher order radial mode is observed. The shifting of the lasing peaks could be due to various reasons such as change of the cavity size,[45] or refractive index of the fiber or matrix.[40,47] However, by bending the fiber to different degrees, there is no significant change of the size of the fiber, which can be seen from Figure S5. This is because the polymer fiber after curing is solid. It is still possible that the cross-sectional shape of the microfiber may change due to strain, but this change should be very small. Based on our lateral investigation, the change of the size of cavity is not the primary cause of the spectral shifts.

It is reported that the refractive index of PDMS is very sensitive to the force and temperature due to its high elasto-optic and thermo-optic coefficients.[48] In ideal case, the bent structure will suffer from both tensile and compressive strain at the outer and inner edges.[49] This corresponds to the situations as indicated in Figure 5g and Figure 5h, respectively. As shown in Figure 5d, based on eq 1, the mode number of the lasing peaks can be identified when $\Delta L = 0$ μm, by considering $r = 1$ and $R = 24$ μm. Therefore, if we return to eq 1 and fix the values of R, r, and m, the resonant wavelength can be described by a function of n_1 and n_2. Considering the main lasing peak TM^1_{374}, the contour plot of resonant wavelength can be

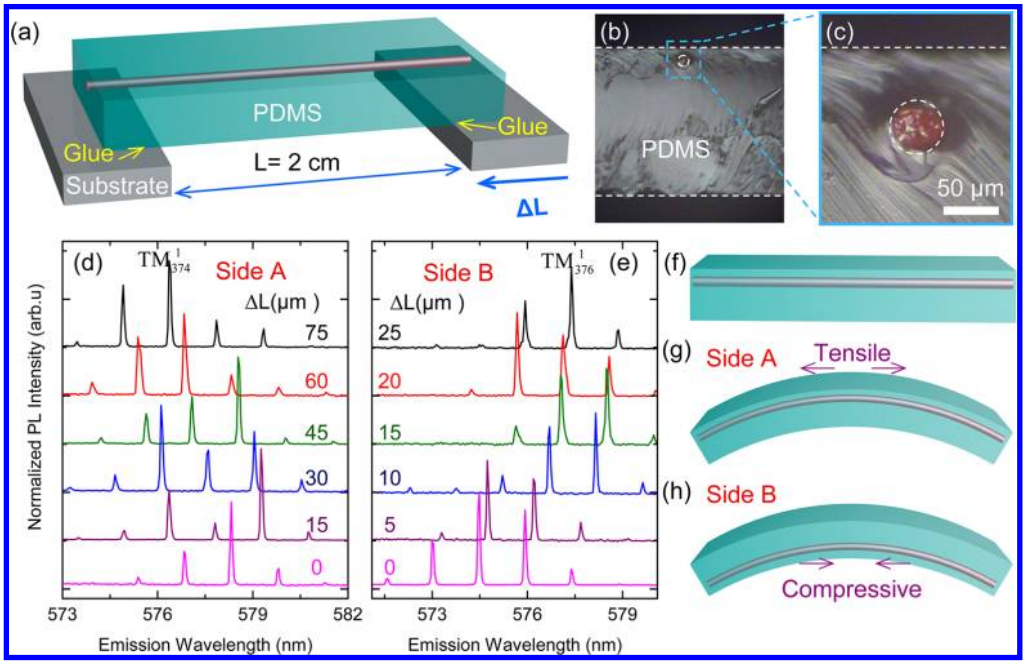

Figure 5. (a) Schematic diagram shows the bending of the fiber inside PDMS elastomer. (b) Cross-section of the fiber inside PDMS and (c) the magnification of the fiber; (d) and (e) are the lasing emission from fiber under different degrees of bending and cases, as schematically shown in (f–h).

dx.doi.org/10.1021/ph400084s | ACS Photonics 2014, 1, 11–16

obtained as Figure 6a, where the axes are the refractive index and the color represent resonant wavelength. The resonant

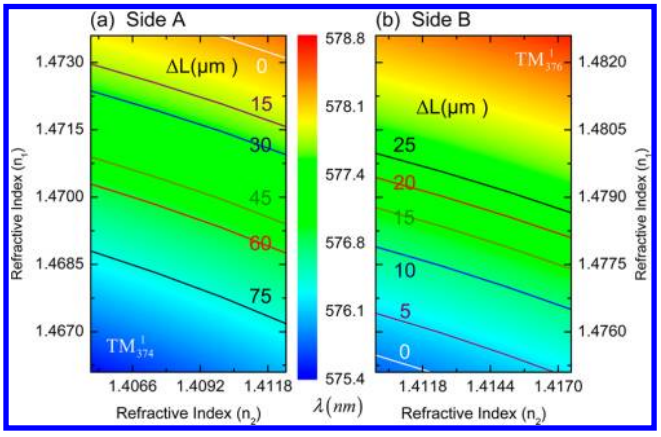

Figure 6. Contour plot of resonant wavelength as a function of refractive index n_1 and n_2, for different cases, namely, Side A (tensile strain) and Side B (compress strain). Solid lines denote the resonant wavelength under different bending situations.

wavelength under different bending situations is traced by solid lines. It is noted that the decrease of refractive index of fiber and PDMS will lead to the blueshift of lasing peaks. This should be reasonable because different strain brings about different refractive index. When Side A is on the top, both fiber and PDMS will suffer from tensile stress. The induced tensile stress intends to "dilute" the materials, which results in the decrease of the refractive index. In contrast, when Side B is on the top, the fiber and PDMS will suffer from compressive strain. Therefore, the lasing peaks demonstrate redshift (Figure 5e) due to the increase of refractive index (Figure 6b). As shown in Figure 6, the scale of refractive index change is only 0.0075 for n_1 and n_2, which indicates the high sensitivity of the lasing peaks to the change of refractive index.[17] It can be clearly seen that bending caused the lasing peaks shift to either a short or long wavelength depending on different types of strain. Following this idea, various kinds of gain materials can be involved, which is effective to extend the laser emission range and tune it to desired positions.

In conclusion, we have exploited the fabrication of polymer microfiber in flexible PDMS elastomer. Optical-pumped WGM lasing with enhanced photostability was achieved. Due to the flexibility of the PDMS elastomer, mechanical tuning of WGM lasing from the fiber was achieved. It is found that the WGM lasing was very sensitive to the refractive index of fiber and PDMS matrix. Bidirectional tuning of the lasing peaks was realized by different types of strain. Our method provides an effective method to protect the fiber against photo-oxidation. The demonstration of bending-induced lasing tuning may help to advance photonic and sensing devices based on polymer fibers.

■ ASSOCIATED CONTENT

Supporting Information

Additional information of the schematic optical setup for measurement, FESEM images of the microfiber, PL spectrum of the microfiber around lasing threshold, and optical image of microfiber with different sizes and under bending. This material is available free of charge via the Internet at http://pubs.acs.org.

■ AUTHOR INFORMATION

Corresponding Author

*E-mail: hdsun@ntu.edu.sg.

Notes

The authors declare no competing financial interest.

■ ACKNOWLEDGMENTS

Supports from the Singapore Ministry of Education through the Academic Research Fund (Tier 1) under Project No. RG63/10 and from the Singapore National Research Foundation through the Competitive Research Programme (CRP) under Project Nos. NRF-CRP5-2009-04 and NRF-CRP6-2010-02 are gratefully acknowledged.

■ REFERENCES

(1) Reithmaier, J. P.; Sek, G.; Loffler, A.; Hofmann, C.; Kuhn, S.; Reitzenstein, S.; Keldysh, L. V.; Kulakovskii, V. D.; Reinecke, T. L.; Forchel, A. Strong Coupling in a Single Quantum Dot-Semiconductor Microcavity System. *Nature* **2004**, *432*, 197−200.

(2) Chen, R.; Sun, H. D.; Wang, T.; Hui, K. N.; Choi, H. W. Optically Pumped Ultraviolet Lasing from Nitride Nanopillars at Room Temperature. *Appl. Phys. Lett.* **2010**, *96*, 241101.

(3) Samuel, I. D. W.; Turnbull, G. A. Organic Semiconductor Lasers. *Chem. Rev.* **2007**, *107*, 1272−1295.

(4) Strauf, S.; Hennessy, K.; Rakher, M. T.; Choi, Y. S.; Badolato, A.; Andreani, L. C.; Hu, E. L.; Petroff, P. M.; Bouwmeester, D. Self-Tuned Quantum Dot Gain in Photonic Crystal Lasers. *Phys. Rev. Lett.* **2006**, *96*, 127404.

(5) Cao, H.; Zhao, Y. G.; Ho, S. T.; Seelig, E. W.; Wang, Q. H.; Chang, R. P. H. Random Laser Action in Semiconductor Powder. *Phys. Rev. Lett.* **1999**, *82*, 2278−2281.

(6) Chen, R.; Bakti Utama, M. I.; Peng, Z.; Peng, B.; Xiong, Q.; Sun, H. Excitonic Properties and Near-Infrared Coherent Random Lasing in Vertically Aligned CdSe Nanowires. *Adv. Mater.* **2011**, *23*, 1404−1408.

(7) Chen, R.; Ye, Q.-L.; He, T.; Ta, V. D.; Ying, Y.; Tay, Y. Y.; Wu, T.; Sun, H. Exciton Localization and Optical Properties Improvement in Nanocrystal-Embedded ZnO Core−Shell Nanowires. *Nano Lett.* **2013**, *13*, 734−739.

(8) Gargas, D. J.; Moore, M. C.; Ni, A.; Chang, S.-W.; Zhang, Z.; Chuang, S.-L.; Yang, P. Whispering Gallery Mode Lasing from Zinc Oxide Hexagonal Nanodisks. *ACS Nano* **2010**, *4*, 3270−3276.

(9) Chen, R.; Ling, B.; Sun, X. W.; Sun, H. D. Room Temperature Excitonic Whispering Gallery Mode Lasing from High-Quality Hexagonal ZnO Microdisks. *Adv. Mater.* **2011**, *23*, 2199.

(10) Zhang, C.; Zou, C.-L.; Yan, Y.; Wei, C.; Cui, J.-M.; Sun, F.-W.; Yao, J.; Zhao, Y. S. Self-Assembled Organic Crystalline Microrings as Active Whispering-Gallery-Mode Optical Resonators. *Adv. Opt. Mater.* **2013**, *1*, 357−361.

(11) Nezhad, M. P.; Simic, A.; Bondarenko, O.; Slutsky, B.; Mizrahi, A.; Feng, L.; Lomakin, V.; Fainman, Y. Room-Temperature Subwavelength Metallo-Dielectric Lasers. *Nat. Photonics* **2010**, *4*, 395−399.

(12) Ma, R. M.; Oulton, R. F.; Sorger, V. J.; Bartal, G.; Zhang, X. Room-Temperature Sub-Diffraction-Limited Plasmon Laser by Total Internal Reflection. *Nat. Mater.* **2011**, *10*, 110−113.

(13) Zhou, W.; Dridi, M.; Suh, J. Y.; Kim, C. H.; Co, D. T.; Wasielewski, M. R.; Schatz, G. C.; Odom, T. W. Lasing Action in Strongly Coupled Plasmonic Nanocavity Arrays. *Nat. Nanotechnol.* **2013**, *8*, 506−511.

(14) Suh, J. Y.; Kim, C. H.; Zhou, W.; Huntington, M. D.; Co, D. T.; Wasielewski, M. R.; Odom, T. W. Plasmonic Bowtie Nanolaser Arrays. *Nano Lett.* **2012**, *12*, 5769−5774.

(15) Kasprzak, J.; Richard, M.; Kundermann, S.; Baas, A.; Jeambrun, P.; Keeling, J. M. J.; Marchetti, F. M.; Szymanska, M. H.; Andre, R.; Staehli, J. L.; Savona, V.; Littlewood, P. B.; Deveaud, B.; Dang, L. S.

Bose-Einstein Condensation of Exciton Polaritons. *Nature* **2006**, *443*, 409−414.
(16) Humar, M.; Musevic, I. 3D Microlasers from Self-Assembled Cholesteric Liquid-Crystal Microdroplets. *Opt. Express* **2010**, *18*, 26995−27003.
(17) Vollmer, F.; Arnold, S. Whispering-Gallery-Mode Biosensing: Label-Free Detection Down to Single Molecules. *Nat. Methods* **2008**, *5*, 591−596.
(18) Vahala, K. J. Optical Microcavities. *Nature* **2003**, *424*, 839−846.
(19) McCall, S. L.; Levi, A. F. J.; Slusher, R. E.; Pearton, S. J.; Logan, R. A. Whispering-Gallery Mode Microdisk Lasers. *Appl. Phys. Lett.* **1992**, *60*, 289−291.
(20) Reitzenstein, S.; Forchel, A. Quantum Dot Micropillars. *J. Phys. D: Appl. Phys.* **2010**, *43*, 033001.
(21) Ta, V. D.; Chen, R.; Sun, H. D. Tuning Whispering Gallery Mode Lasing from Self-Assembled Polymer Droplets. *Sci. Rep.* **2013**, *3*, 1362.
(22) Schäfer, J.; Mondia, J. P.; Sharma, R.; Lu, Z. H.; Susha, A. S.; Rogach, A. L.; Wang, L. J. Quantum Dot Microdrop Laser. *Nano Lett.* **2008**, *8*, 1709−1712.
(23) Ta, V. D.; Chen, R.; Sun, H. D. Self-Assembled Flexible Microlasers. *Adv. Mater.* **2012**, *24*, OP60−OP64.
(24) Chen, R.; Ta, V. D.; Sun, H. D. Single Mode Lasing from Hybrid Hemispherical Microresonators. *Sci. Rep.* **2012**, *2*, 244.
(25) Haase, J.; Shinohara, S.; Mundra, P.; Risse, G.; Lyssenko, V. G.; Frob, H.; Hentschel, M.; Eychmuller, A.; Leo, K. Hemispherical Resonators with Embedded Nanocrystal Quantum Rod Emitters. *Appl. Phys. Lett.* **2010**, *97*, 211101.
(26) Zhao, Y. S.; Peng, A.; Fu, H.; Ma, Y.; Yao, J. Nanowire Waveguides and Ultraviolet Lasers Based on Small Organic Molecules. *Adv. Mater.* **2008**, *20*, 1661−1665.
(27) O'Carroll, D.; Lieberwirth, I.; Redmond, G. Melt-Processed Polyfluorene Nanowires as Active Waveguides. *Small* **2007**, *3*, 1178−1183.
(28) Gu, F.; Yu, H.; Wang, P.; Yang, Z.; Tong, L. Light-Emitting Polymer Single Nanofibers Via Waveguiding Excitation. *ACS Nano* **2010**, *4*, 5332−5338.
(29) O'Carroll, D.; Lieberwirth, I.; Redmond, G. Microcavity Effects and Optically Pumped Lasing in Single Conjugated Polymer Nanowires. *Nat. Nanotechnol.* **2007**, *2*, 180−184.
(30) Ta, V. D.; Chen, R.; Ma, L.; Ying, Y. J.; Sun, H. D. Whispering Gallery Mode Microlasers and Refractive Index Sensing Based on Single Polymer Fiber. *Laser Photon. Rev.* **2013**, *7*, 133−139.
(31) Ta, V. D.; Chen, R.; Sun, H. D. Coupled Polymer Microfiber Lasers for Single Mode Operation and Enhanced Refractive Index Sensing. *Adv. Opt. Mater.* **2013**, DOI: 10.1002/adom.201300433.
(32) Klimov, V. I.; Ivanov, S. A.; Nanda, J.; Achermann, M.; Bezel, I.; McGuire, J. A.; Piryatinski, A. Single-Exciton Optical Gain in Semiconductor Nanocrystals. *Nature* **2007**, *447*, 441−446.
(33) Klimov, V. I.; Mikhailovsky, A. A.; Xu, S.; Malko, A.; Hollingsworth, J. A.; Leatherdale, C. A.; Eisler, H.-J.; Bawendi, M. G. Optical Gain and Stimulated Emission in Nanocrystal Quantum Dots. *Science* **2000**, *290*, 314−317.
(34) Moon, H. J.; Chough, Y. T.; Kim, J. B.; An, K.; Yi, J.; Lee, J. Cavity-Q-Driven Spectral Shift in a Cylindrical Whispering-Gallery-Mode Microcavity Laser. *Appl. Phys. Lett.* **2000**, *76*, 3679−3681.
(35) Humar, M.; Ravnik, M.; Pajk, S.; Musevic, I. Electrically Tunable Liquid Crystal Optical Microresonators. *Nat. Photonics* **2009**, *3*, 595−600.
(36) Wallikewitz, B. H.; Nikiforov, G. O.; Sirringhaus, H.; Friend, R. H. A Nanoimprinted, Optically Tuneable Organic Laser. *Appl. Phys. Lett.* **2012**, *100*, 173301.
(37) Li, Z.; Zhang, Z.; Scherer, A.; Psaltis, D. Mechanically Tunable Optofluidic Distributed Feedback Dye Laser. *Opt. Express* **2006**, *14*, 10494−10499.
(38) Saito, M.; Shimatani, H.; Naruhashi, H. Tunable Whispering Gallery Mode Emission from a Microdroplet in Elastomer. *Opt. Express* **2008**, *16*, 11915−11919.
(39) Song, W.; Psaltis, D. Pneumatically Tunable Optofluidic Dye Laser. *Appl. Phys. Lett.* **2010**, *96*, 081101.
(40) Lu, T.-W.; Chiu, L.-H.; Lin, P.-T.; Lee, P.-T. One-Dimensional Photonic Crystal Nanobeam Lasers on a Flexible Substrate. *Appl. Phys. Lett.* **2011**, *99*, 071101.
(41) Saito, M.; Koyama, K. Deformable Microdroplet Cavity Fabricated by an Inkjet Method. *Jpn. J. Appl. Phys.* **2010**, *49*, 092501.
(42) Görrn, P.; Lehnhardt, M.; Kowalsky, W.; Riedl, T.; Wagner, S. Elastically Tunable Self-Organized Organic Lasers. *Adv. Mater.* **2011**, *23*, 869−872.
(43) Nazzal, A. Y.; Wang, X.; Qu, L.; Yu, W.; Wang, Y.; Peng, X.; Xiao, M. Environmental Effects on Photoluminescence of Highly Luminescent CdSe and CdSe/Zns Core/Shell Nanocrystals in Polymer Thin Films. *J. Phys. Chem. B* **2004**, *108*, 5507−5515.
(44) Lam, C. C.; Leung, P. T.; Young, K. Explicit Asymptotic Formulas for the Positions, Widths, and Strengths of Resonances in Mie Scattering. *J. Opt. Soc. Am. B* **1992**, *9*, 1585−1592.
(45) Tang, S. K. Y.; Derda, R.; Quan, Q.; Lončar, M.; Whitesides, G. M. Continuously Tunable Microdroplet-Laser in a Microfluidic Channel. *Opt. Express* **2011**, *19*, 2204−2215.
(46) Yim, T.-J.; Zentgraf, T.; Min, B.; Zhang, X. All-Liquid Photonic Microcavity Stabilized by Quantum Dots. *J. Am. Chem. Soc.* **2010**, *132*, 2154−2156.
(47) Aas, M.; Jonáš, A.; Kiraz, A. Lasing in Optically Manipulated, Dye-Doped Emulsion Microdroplets. *Opt. Commun.* **2013**, *290*, 183−187.
(48) Markos, C.; Vlachos, K.; Kakarantzas, G. Bending Loss and Thermo-Optic Effect of a Hybrid Pdms/Silica Photonic Crystal Fiber. *Opt. Express* **2010**, *18*, 24344−24351.
(49) Chen, R.; Ye, Q.-L.; He, T. C.; Wu, T.; Sun, H. D. Uniaxial Tensile Strain and Exciton-Phonon Coupling in Bent ZnO Nanowires. *Appl. Phys. Lett.* **2011**, *98*, 241916.